Time-shifted Pilot-based Scheduling with Adaptive Optimization for Pilot Contamination Reduction in Massive MIMO

Ambala Pradeep Kumar and Tadisetty Srinivasulu

KU College of Engineering and Technology, Kakatiya University, Warangal, Telangana, India

Abstract—Massive multiple-input multiple-output (MIMO) is considered to be an emerging technique in wireless communication systems, as it offers the ability to boost channel capacity and spectral efficiency. However, a massive MIMO system requires huge base station (BS) antennas to handle users and suffers from inter-cell interference that leads to pilot contamination. To cope with this, time-shifted pilots are devised for avoiding interference between cells, by rearranging the order of transmitting pilots in different cells. In this paper, an adaptive-elephant-based spider monkey optimization (adaptive ESMO) mechanism is employed for time-shifted optimal pilot scheduling in a massive MIMO system. Here, user grouping is performed with the sparse fuzzy c-means (Sparse FCM) algorithm, grouping users based on such parameters as large-scale fading factor, SINR, and user distance. Here, the user grouping approach prevents inappropriate grouping of users, thus enabling effective grouping, even under the worst conditions in which the channel operates. Finally, optimal time-shifted scheduling of the pilot is performed using the proposed adaptive ESMO concept designed by incorporating adaptive tuning parameters. The efficiency of the adaptive ESMO approach is evaluated and reveals superior performance with the highest achievable uplink rate of 43.084 bps/Hz, the highest SINR of 132.9 dB, and maximum throughput of 2.633 Mbps.

Keywords—massive MIMO, pilot contamination, sparse FCM, time-shifted pilot scheduling, user grouping.

1. Introduction

The advancement of big data and the demand for communication networks has increased considerably, meaning that classical wireless networks, such as 4G, are not able to meet the demand of network users [1]. Massive MIMO is a fundamental technique for establishing 5G wireless communications and maximizing spectral efficiency. It offers the ability to deploy different communication models, like cooperative communication, orthogonal frequency division multiplexing (OFDM), and multicarrier communication. Massive MIMO relies on varying frequencies in the frequency division duplex (FDD) mode. Thus, massive MIMO is based on the time division duplex (TDD) system [2], which utilizes channel reciprocity for obtaining the channel state information (CSI) [3] required. However, as anticipated, the lower coherence interval limits the count of orthogonal pilots assigned to a user. The use of similar pilots by various cell users means that pilot contaminations cannot be distinguished at the base station (BS). Furthermore, massive MIMO has acquired much interest because of gains in energy and spectrum efficiency affecting BS with huge antennas that serve a set of users concurrently [4]. Under multi-cell scenarios, inevitable reuse of pilots in varying cells is experienced and channel estimates generated from certain cells are prejudiced by the reused pilots which are then sent by users from other cells. The phenomenon is termed as pilot contamination [5].

Despite its potential, the massive MIMO model poses various limitations. One of them is the effect of pilot contamination. The problem occurs when users of adjoining cells utilize similar sequences of pilots. The most unpleasant cases are supposed to occur when neighboring cells transmit similar sequences of a pilot at a similar time. For avoiding the issue of synchronized pilots between adjoining cells, a time-shifted pilot method is devised in which some of the cells transmits downlink data, whereas others send pilots. This technique enhances transmission rates of the system. However, the assessment is based on the supposition that the number of antennas at BS is unlimited. Due to the infinite number of antennas, some interference may be considered to be negligible [6]. Pilot contamination unavoidably limits the efficiency of a huge-scale antenna of a massive MIMO model, because of the corrupted estimation of channels. The recycling of frequency amongst adjacent cells led to interference that limited the quality of service offer to cellular users, especially those positioned at cell edges. Service providers look for solutions to restore performance at low SINR cell locations. Numerous methods are devised to mitigate inter-cell interference.

Among these are solutions that rely on multiple antennas, meaning that on the BS side, these arrays become more affordable [7].

In the literature, various methods are devised to mitigate the effects of pilot contamination. The greedy pilot allocation technique allows to alleviate the effect of contaminating pilots by using arithmetical channel covariance information, but still suffers from a number of complications. A blind technique using subspace partition [8] is used for minimizing inter-cell interference (ICI), wherein channel vectors of different users are supposed orthogonal. An adaptive pilot clustering technique [9] is devised based on coalitional game theory. It may alleviate pilot contamination by employing a subset of pilot resources in an individual cell, thus causing spectral efficiency loss. In [10], the pilot contamination precoding (PCP) method is devised, wherein a precoding matrix is using zero-forcing (ZF) for obtaining an infinite signal-to-interference plus noise ratio (SINR), but it affects entire systems. In [11], an optimal technique for determining a simple suboptimal algorithm and an optimum pilot contamination precoding matrix are devised. In paper [12], an intelligent pilot allocation method is devised that could increase uplink SINR of every user in a target cell with large-scale fading. The pilot power control method shown in [13], [14] is devised for classified cells and allows to minimize pilot contamination, improve downlink reachability and foster efficiency of the entire system.

In [15], a ZF time-shifted pilot scheme is utilized for alleviating pilot contamination by using conjugate beamforming. In [16], the interference cancelation (IC) precoding method is devised for mitigating pilot contamination in massive MIMO models. The method improves service quality and allows for effective user scheduling. In [17], a pilot contamination reduction method is devised that is based on complicated exponentials. In this paper, linear time-varying (LTV) channels are evaluated with optimum pilot symbols and they are devised using minimum mean square error (MMSE) criteria. It is proved that the optimum pilot method is capable of setting successive pilot tones and allocating all pilot clusters uniformly within the frequency domain.

The goal is to use time-shifted pilots for mitigating pilot contamination, and thereby assuring effective pilot scheduling in massive MIMO. The motive of the proposed scheduling technique is to utilize time-shifted pilots to initiate pilot scheduling. Initially, user grouping is performed based on an algorithm that gather users as center and edge user groups, depending on various pilot contamination levels. The grouping of users is performed using sparse FCM, based on attributes that involve large-scale fading factors, SINR and user distance in such a way that inappropriate grouping of users is prevented, enabling effective grouping even under the worst channel conditions. Then, pilot scheduling is performed based on the proposed adaptive ESMO algorithm designed by incorporating adaptive tuning parameters in the ESMO algorithm.

The major contribution of the research performed is to devise an approach enabling time-shifted optimal scheduling of pilots using the adaptive ESMO algorithm that is designed by combining adaptive tuning parameters with ESMO.

The remaining sections of the paper are arranged in the following manner: Section 2 elaborates on the description of conventional pilot scheduling strategies and on the challenges faced. The model of a massive MIMO system is illustrated in Section 3. The proposed method for time-shifted pilot scheduling is portrayed in Section 4. Outcomes of the proposed strategy and its comparisons with other methods are depicted in Section 5. Section 6 presents the conclusions.

2. Literature Survey

Akgun *et al.* devised, in [18], an attack model in which the foe infected the uplink pilot transmissions of multiple users, i.e. they conducted a pilot contamination attack. The downlink transmission rates with/without the attack were derived by exploiting the channel hardening effect of massive MIMO. This model did not consider attack models that involved multiple frequencies and time slots. Wu *et al.* in [19] devised secure communication for the time duplex MIMO model, considering eavesdropping. The eavesdropper attacked the transmission of the uplink pilot before eavesdropping on downlink transmissions. Moreover, pilot signals and data signals were utilized for estimating the uplink channel. This method maximized the asymptotic estimation error and suffered from loss of performance. Fan *et al.* in [20] devised a fractional pilot reuse (FPR) mechanism for minimizing the contamination of pilots from the massive MIMO model. In FPR, users are split into the center and edges of the cell. Then, cell users utilize orthogonal pilots for preventing interference caused by adjoining cells, meanwhile the cell center reutilizes similar pilots for enhancing the efficiency of pilots. The throughput of the network was influenced by the count of service users and pilots.

Saraereh *et al.* in [21] presented a method deployed in a massive MIMO model for decontaminating the set of pilot sequences. The first step is based on path loss to perform grouping, and the second step is based on the pseudo-random code. However, the method failed to consider pilot contamination in sectoral cells. Shaalan *et al.* [22] developed two pilot assignment methods for minimizing the impact of pilot contamination. Time-shifted pilot assignment (TSPA) method were utilized, splitting the cellular network into different groups in which users belonging to the same group were transmitted to uplink-pilots, whereas others received downlink data. Also, the heuristic weighted graph coloring-based pilot assignment (WGC-PA) method was utilized for minimizing intra-group interference. The method showed that two consecutive cells belong to the same group in the time-shifted method. Hua and Chang in [23] devised a "cocktail" method for com-

bining two classic countermeasures, namely time-shifted pilots (TSP) and fractional pilot reuse methods for addressing the issue of pilot contamination in a full-duplex massive MIMO model. The TSP method was adapted for duplicating inner cell regions, such that the count of gathered users is twofold. Also, the base station must function in the full-duplex mode and the symbols of the pilot are employed for attaining the user diversity gain. The outcomes of the simulation verified the accuracy and enhanced the overall uplink and downlink rates. Salh *et al.* [24] developed a channel estimation method which relied on comprehensive knowledge of huge-scale expansion by adapting the orthogonal pilot sequence for eliminating pilot contamination among edge users with minimized channel quality losses, using huge-scale fading. Channel quality available to users was improved. The performance of the methods was analyzed and it was shown that performance losses were minimized, with better channel approximation leading to elevated data rates. However, the method was unable to deal with complex signal processing methods. Wei *et al.* [25] devised a method using time-shifted pilots based on joint position-power optimization for massive MIMO. Here, an effective user scheduling strategy was applied for optimizing pilot power, using the average power constraint. Furthermore, the power and the positions of pilots were optimized iteratively. The analysis performed revealed that the method offered substantial coordination gains in terms of performance, based on spectral efficiency.

2.1. Research Challenges

The research challenges confronted by the conventional time-shifted pilot-based scheduling schemes are:

- in [22], the time-shifted pilot assignment (TSPA) method is devised for reducing the impacts of pilot contamination. However, the TSPA method suffered from intra-group interference that occurred between the cells of similar groups, and offered no approach to grouping cells and to tackling pilot-to-downlink data interference. Moreover, there is a lack of perfect synchronization between cells;

- in massive MIMO-TDD models, the BS obtains CSI using uplink pilots sent by the user with channel reciprocity. However, owing to lower coherence time rates, the reuse of pilots from user terminals in a different cell is foreseeable, which results in pilot contamination issues. Thus, the evaluation of CSI is correlated and produced imprecise beamforming signals [25];

- in massive MIMO-TDD models, the BS obtains CSI using the uplink pilots sent by the user with channel reciprocity. However, owing to less coherence time, the reuse of pilots from user terminals in a different cell is foreseeable, which results in a pilot

contamination issue. Thus, the evaluation of CSI is correlated and produced imprecise beamforming signals [25];

- the major issue in massive MIMO is related to pilot contamination effects impacting channel estimation. Pilot contamination leads to inaccurate channel estimation in 5G downlink transmissions. Besides, various issues need to be faced while executing a massive MIMO model that included noise contamination affecting spectral efficiency.

3. System Model

Massive MIMO is a fundamental element of upcoming applications of 5G networks. MIMO is a wireless network that permits the transmission and reception of large amounts of data signals at the same time and via the same radio channels. In order to satisfy the high data rates and to ensure improved service quality, massive MIMO is favored as it relies on huge antennas at access points. Figure 1 illustrates a massive MIMO model with pilot contamination in the uplink transmission. It comprises antenna arrays, base stations (BS), and different user terminals. The BS sends data packets from various antennas to different terminals at a similar frequency. Massive MIMO [21] is adopted to offer enhanced coverage, high energy efficiency and high data rates. However, various performance restricting issues need to be confronted in this approach in connection with channel estimation and pilot design.
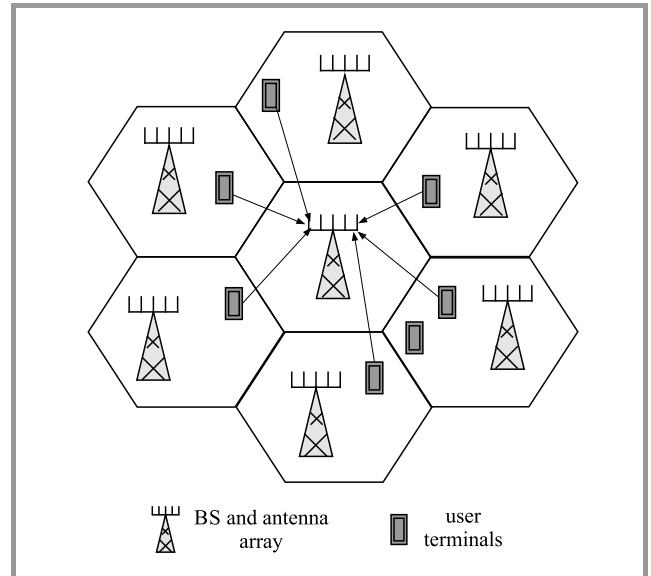
Fig. 1. Model of a massive MIMO system with uplink transmission pilot contamination.

Thus, an effective method is devised for eliminating pilot contamination in order to solve pilot-related problems. It stems from Fig. 1 that each hexagonal cell utilizes the central BS associated with A antennas for D users ($D \gg A$).

Thus, the channel propagation matrix for every user in the cell communicating with the cell site is:

$$b_{def} = a_{def}\sqrt{C_{def}} , \qquad (1)$$

where a_{def} indicates the small scale fading vector, $C_{def} = d(d_{def1}, c_{def2}, c_{def3}, \ldots, c_{defK})$ is a $K \times K$ order diagonal matrix that describes the large-scale fading factor of each user to the BS of e-th cell. The large-scale fading factor of f-th user of e-th cell to BS of d-th cell is:

$$c_{defK} = \left(\frac{M_{defK}}{\frac{k_{defK}}{N}} \right)^{\eta} , \qquad (2)$$

where M_{defK} describes shadow fading, k_{defK} is the distance evaluated between f-th user in e-th cell and BS in d-th cell, N represents the radius of the cell, and η is the path loss factor.

The channel vector is given by a constant at coherence time and varies autonomously in varying intervals. Here, the BS produces a downlink channel based on the uplink pilot sequence in coherence time. When data is sent, all users send uplink data to the BS and get downlink at d-th cell as:

$$s_d^u = \sqrt{K_u} \sum_{e=1}^{T} \sum_{f=1}^{D} b_{def} x_{ef}^u + v_d^u , \qquad (3)$$

where symbol sent from f-th user in e-th cell is x_{ef}^u with $\varepsilon\{|x_{ef}^u|^2\} = 1$, and uplink is K_u.

Let $\theta_d = (\theta_1, \theta_2, \ldots, \theta_D)^D$ be the pilot sequence matrix of all users in the e-th cell, which satisfies $\theta_d \theta_d^R = X_D$. The pilot sequence matrix received in BS at d-th cell is:

$$s_d^t = \sqrt{N_t}\left(\sum_{d=1}^{T} b_{def}\theta_D \right) + v_d^u , \qquad (4)$$

where N_t is the pilot signal transmission power and v_d^u is the additive white Gaussian noise matrix. For this scenario, the BS of d-th cell evaluates channel matrix R_{dd} with convolutional channel estimation and is:

$$b_{def}^{\wedge} = \frac{1}{\sqrt{N_t}} s_d^t \theta_d^R = b_{def} + \sum_{e \neq d} b_{def} + \frac{1}{\sqrt{N_t}} v_d^u \theta_d^R . \qquad (5)$$

After the user sends the pilot, every user transmits the data signal to the BS and utilizes the same time frequency resource. The linear blend of channel b_{def} for $1 \leq e \leq T$ is expressed as d_{ddf}, which contains channel users in other cells associated with pilot sequences and is termed pilot contamination. Then, the determined symbol generated from f-th user in d-th cell using a low complexity matched filter detector, offers computed channel matrix $b_{def}^{\wedge}$ given as:

$$\hat{x}_{df}^u = b_{ddf}^R s_d^u , \qquad (6)$$

$$\hat{x}_{df}^u = \left(\sum_{e=1}^{T} b_{def}^F + w_{df}^R \right)\left(\sqrt{K_u} \sum_{e=1}^{T} \sum_{f=1}^{D} d_{def} x_{ef}^u + v_d^u \right) , \qquad (7)$$

$$\hat{x}_{df}^u = \sum_{e=1}^{T} b_{def}^R \cdot \sqrt{K_u} \sum_{e=1}^{T} \sum_{f=1}^{D} b_{def} x_{ef}^u + \rho_{d,f}^u , \qquad (8)$$

$$\hat{x}_{df}^u = \sqrt{K_u}\left(b_{def}^R b_{ddf} x_{df}^u + \sum_{e \neq d} b_{def}^R b_{def} x_{ef}^u \cdot \right) + \rho_{d,f}^u , \qquad (9)$$

$$\hat{x}_{df}^u = A\sqrt{K_u}\left(\alpha_{ddf} x_{df}^u + \sum_{e \neq d} \alpha_{def} x_{ef}^u \cdot \right) + \rho_{d,f}^u , \qquad (10)$$

where w_{dc} indicates f-th column of $\frac{v_d^t \theta_d^R}{\sqrt{s_j}}$ and $\rho_{d,f}^u$ represents orthogonality between channels of many users. When the BS antenna count reaches to infinity, the detected symbol is:

$$x_{df}^u \approx A\sqrt{K_u}\left(\alpha_{ddf} x_{df}^u + \sum_{e \neq m} \alpha_{def} x_{ef}^u \right) . \qquad (11)$$

4. Scheduling Using Adaptive ESMO Algorithm

The proposed scheduling algorithm utilizes time-shifted pilots. At first, the grouping of users is performed based on the user grouping algorithm which assists in grouping users (center user and edge user) based on various levels of contaminating pilots. The grouping of users is performed using sparse FCM, based on such parameters as large-scale fading factor, SINR, and user distance. Finally, pilot scheduling is performed using adaptive ESMO, i.e. a method that combines adaptive tuning parameters with ESMO. Figure 2 shows a schematic view of the time-shifted pilot-based scheduling process using the proposed adaptive ESMO algorithm.

4.1. Grouping of Users with Sparse FCM

Users are divided into different groups in order to minimize the complexity of processing by serving each group individually. In a specific time slot, a subset of users is scheduled within each group for transmission. Additionally, the precise SINR of each user is essential for user grouping. However, in conventional user grouping methods, channel covariance matrices are adopted for grouping users, which causes inter-group interference. Here, user computing parameters and sparse FCM are employed for facilitating the grouping process. The parameters include user distance, SINR, and the large-scale fading factor [21]. These parameters are essential for designing the user grouping method in order to improve system capacity.

The uplink SINR of v-th user in b-th cell is:

$$SINR_{df}^u = \frac{|b_{ddf}^R b_{ddf}|^2}{\sum_{e \neq d} |b_{def}^R b_{def}|^2 + \frac{|\rho_{d,d}^u|^2}{K_u}} , \qquad (12)$$

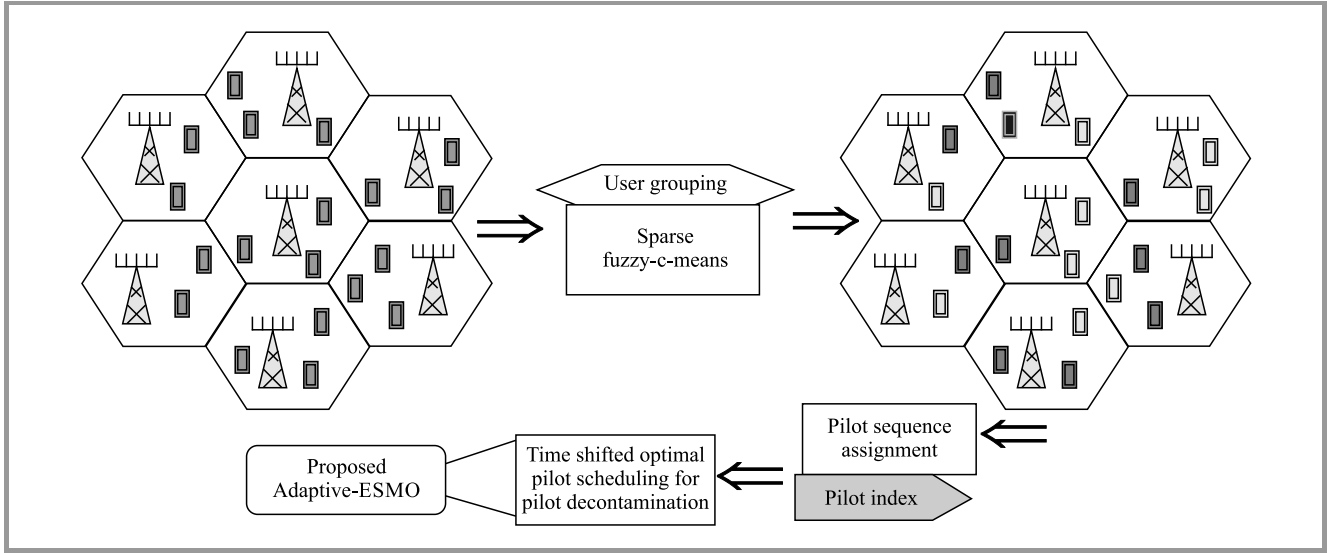With large numbers of BS, the uplink SINR is expressed as:

Fig. 2. Schematic view of the time-shifted pilot-based scheduling using proposed adaptive ESMO.

$$SINR_{df}^u = \frac{\alpha_{ddf}^2}{\sum\limits_{e \neq d} \alpha_{def}^2} \ . \tag{13}$$

Hence, the SINR of the user is expressed as G_1.
The large scaling factor of f-th user of e-th cell to BS of d-th cell is obtained in Eq. (2). This factor is expressed as G_2. User distance is computed between the location of f-th user and the center of the cell:

$$\partial = \sqrt{\sum\limits_{f=1}^{L} \left(\omega_f^{loc}, z^{cell} \right)} \ , \tag{14}$$

where ∂ indicates the user distance, ω_f^{loc} indicates the location of f-th user, z^{cell} represents the center of the cell, and G_3 indicates user distance. Hence, user grouping-related parameters are formulated as:

$$\mathrm{T} = G_1, G_2, G_3 \ . \tag{15}$$

User grouping is performed with sparse FCM – a method that relies on such parameters as large-scale fading factor, SINR, and user distance. The goal of sparse FCM is to group users into center user and edge user categories. In sparse FCM [27], dimensional reduction is essential. Here, the advantage consists in grouping users without any delay, and in reducing the level of complexity caused by the optimization method. The steps of sparse FCM are:

- **Initialization**. The foremost step is to initialize the feature weights, which are:

$$\varpi = \varpi_1^n = \varpi_2^n = \ldots = \varpi_z^n = \frac{1}{\sqrt{z}} \ , \tag{16}$$

where z indicates features and n-th attribute weights based on z-th feature indicated as ω_z^n;

- **Update the partition matrix**. Set cluster centers and attribute weights as q and ω. The constraint is $\vartheta(W)$, which must be reduced to:

$$\omega_{ic} = \begin{cases} \dfrac{1}{I_c} & \text{if } r_{ic} \text{ and} \\ & I_c = \text{cardinality}\{e : r_{ic} = 0\} \\ 0 & \text{if } r_{ic} \neq 0 \text{ but } r_{iy} = 0 \\ & \text{for some } y, \, y \neq l \\ \dfrac{1}{\sum\limits_{y=1}^{o} \left(\frac{r_{ic}}{r_{yc}} \right)^{\left(\frac{1}{\gamma-1}\right)}} & \text{otherwise} \end{cases}, \tag{17}$$

where $r_{ic} = \sum\limits_{c=1}^{o} \varpi_e (\upsilon_{ei} - k_{ci})^2$ and cardinality(U) represent cardinality of set U.

The distance measure is r_{ic} which indicates the distance between i-th node and c-th cluster center;

- **Determine cluster centers**. For evaluating cluster centers, it is important to set attribute weight ω and data matrix Z, and estimation of cluster center is:

$$y_{ce} = \begin{cases} 0 & \text{if } \varpi_e = 0 \\ \dfrac{\sum\limits_{i=1}^{n} \omega_{ic}^{\gamma} \upsilon_{ei}}{\sum\limits_{i=1}^{n} \omega_{ic}^{\gamma}} & \text{if } \varpi_e \neq 0 \end{cases}, \tag{18}$$

where $c = 1, \ldots, v$ and $e = 1, \ldots, d$. The c index indicates the cluster center and e represents data attribute. The evaluation of the cluster center is done based on attribute weight ϖ_e. The response of e-th

feature to the objective function is indicated as ϖ_e and constant Y symbolizes dissimilarity measure;

- **Derive the class**. The class is determined using specified clusters $y = \{y_1, y_2, \ldots, y_c, \ldots, y_o\}$ having a membership ω. Class Y_e is detected with the use of an objective function:

$$\max_{\varpi} \sum_{e=1}^{z} \varpi_e . Y_e \, , \tag{19}$$

such that $\|\varpi\|_2^2 \leq 1$, $\|\varpi\|_\kappa^\kappa \leq \lambda$ produces ϖ^*, where λ indicates tuning parameter $(0 \leq \kappa \leq 1)$ and $\|\omega\|_\kappa^\kappa = \sum_{e=1}^{d} |\varpi_e|^\kappa$;

- **Terminate**. The iteration is repeated until the maximum count is reached. The stopping criterion is:

$$\frac{\sum\limits_{e=1}^{z} |\varpi_e^* - \varpi_e^o|}{\sum\limits_{e=1}^{z} |\varpi_e^o|} < 10^{-4} \, . \tag{20}$$

Hence, the count of users in the individual cell is chosen vibrantly. The proposed user grouping approach mitigates inapt grouping of users and facilitates effective grouping even under the worst channel conditions.

Based on the clustering result, the distance attribute of the centroid having the minimum value is considered. The corresponding user belongs to center users (group 1), and the remaining user belongs to edge users (group 2) or nearby edge users (group 3).

4.2. Time-shifted Optimal Pilot Scheduling

Time-shifted pilot slot allocation using the adaptive ESMO method is devised for alleviating impacts of contaminating pilots. The method relies on four time-based scheduling phases, including pilot sequence transmission, processing and estimation of the channel at BS, uplink data transmission, and downlink data transmission. This method assigns pilots to cells at different time-shifted slots. Non-overlapping time slots are assigned to the transmission of pilots by shifting pilot locations. Thus, the use of time-shifting is controlled effectively, without any overlaps, and pilot contamination is removed entirely. A brief illustration of the proposed adaptive ESMO used for time-shifted pilot slot allocation is given below.

The goal of solution encoding is to produce a solution vector using the proposed optimization technique. The solution consists of pilots that match the proposed adaptive ESMO method (Fig. 3). The count of pilots is chosen based on a matrix, wherein the count of users is indicated in a row-wise manner and the count of cells is indicated in a column-wise manner. Let us assume that the total number users is U, the count of groups is G and the count of cells is A. Then, the dimension of the solution is indicated as $A \times G$. Based on the matrix, a solution vector is described

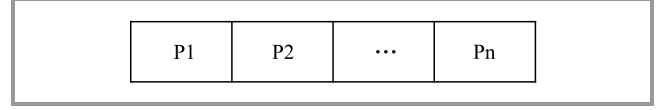that indicates the count of pilots, and its size is represented as $(A \times G)$.

P1	P2	$\cdots$	Pn

Fig. 3. Solution encoding to pilot assignment.

Let us assume that $U = 6$, $G = 3$, and $A = 2$. Let the number of pilots be 2, meaning that pilot length becomes 2. The dimension of the solution is $2(A)$. Figure 4 shows an example of the pilot assignment process.
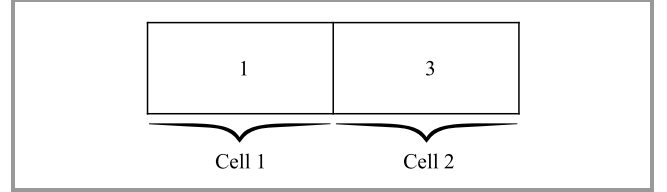
1	3
Cell 1	Cell 2

Fig. 4. Example of pilot assignment process.

Pilot p_1, p_2 is assigned to cell 1 with the index of 1 and 3. The mapping of the above solution in the concept model using a time-shifted pilot sequence is illustrated in Fig. 5. Let us assume that $P, D, U = \{2, 4, 4\}$, where P indicates the total number of pilots, D denotes the downlink scenario and U is an uplink scenario. Then, the solution matrix is represented as:
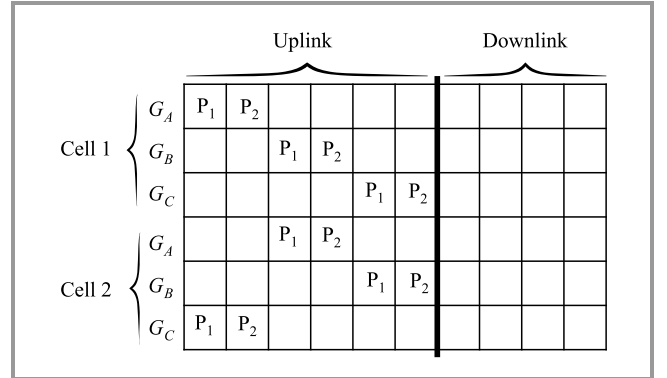
		Uplink				Downlink			
Cell 1	G_A	P_1	P_2						
	G_B			P_1	P_2				
	G_C					P_1	P_2		
Cell 2	G_A			P_1	P_2				
	G_B					P_1	P_2		
	G_C	P_1	P_2						

Fig. 5. Example of the time-shifted pilot sequence.

The level of fitness helps reveal solution quality worked out with the use of the achievable sum rate. It is modeled as a maximization function and is derived below.

The utility function describes the achievable uplink rate, wherein the pilot sequence θ_v is assigned to the E_f-th user:

$$\Theta(E_f, \theta_f) = P_{E_f}^u(E_f, \theta_f) \, , \tag{21}$$

where pilot sequence θ_f allocated to user E_f is expressed as $(E_f, \theta_f) \{W_v : v = 1, \ldots, D!\}$ represents all pilot assignment possibilities, and $W_v = [W_v^1, W_v^2, \ldots, W_v^D]$ indicates v-th assignment. Furthermore, the goal of massive MIMO

is to enhance the achievable target cell sum rate, which is the main optimization issue and is given by:

$$Z : \max_{\{W_v\}} \left\{ \sum_{D=1}^{E} P_{E_f}^u \left(E_f, \theta_{W_u^v} \right) \right\} . \quad (22)$$

The enhanced achievable uplink rate is:

$$P(E, \theta) = (1 - \mu_0) \left\{ \log_2 \left[1 + \text{SINR}(E, \theta) \right] \right\} + \mu_0 \times \sum_{a=1}^{n} B_a , \quad (23)$$

where $\text{SINR}(E, \theta)$ indicates SINR value θ at user E and he transmit power of pilot is expressed as B_a. The total pilot is indicated as a. ESMO provides a solution to the optimization issue by offering optimum pilot assignments.

4.3. Steps of Proposed Adaptive ESMO

Time-shifted optimal pilot scheduling is performed using the proposed adaptive ESMO algorithm which is a combination of ESMO and adaptive tuning parameters. Here, ESMO is determined by integrating EHO from [31] and SMO [39]. The issues of EHO are addressed with SMO that tends to offer a better convergence rate by generating a globally optimized solution. Such a method is simple and may effectively manage several local optima, significant nonlinearity, ruggedness, and interdependence. Additionally, it paves the way to increasing robustness of the optimization technique.

In the self-adaptive method, selection of the learning strategy and control parameters is not required beforehand, and parameter settings self-adapt based on the learning experience. Thus, the incorporation of adaptive concepts into the ESMO algorithm improves the overall performance. The steps of the proposed adaptive ESMO algorithm are as follows:

Initialization. The initialization of the solutions in the search space is:

$$S = \left\{ S_1, S_2, \ldots, S_\kappa, \ldots, S_\ell \right\} , \quad (24)$$

where S_κ indicates κ-th solution, and ℓ is the total number of solutions.

Evaluation of fitness function. The optimum solution is detected using the fitness function. The solution with maximum fitness is chosen as optimal.

Determination of update solution. After computing their fitness, the solutions update ESMO, which enhances the performance of the algorithm as far as discovering optimal pilots is concerned:

$$S_{e,f}(y+1) \left[\frac{[\mu - 1] \left[S^*(y) - S_{e,f}(y) \right]}{\mu \times \left[S^*(y) - S_{e,f}(y) \right]} \right] =$$

$$S_{e,f}(y) - \frac{S_{e,f}(y) \left[S^*(y) - S_{e,f}(y) \right]}{\mu \times \left[S^*(y) - S_{e,f}(y) \right]} +$$

$$T(-1, 1) \times \left[S_{o,f}(y) - S_{e,f}(y) \right] , \quad (25)$$

where $S_{e,f}(y)$ indicates the f dimension of e-th SM, $S_{e,f}(y)$ refers to the f dimension of o-th SM, the random number is denoted as $T(-1, 1)$, $S^*(y)$ signifies the best solution, and μ denotes the scale factor ranging from 0 to 1.

The update is performed using the ESMO algorithm by making the constants self-adaptive in ESMO. To incorporate the adaptive concept, μ is made self-adaptive, such as:

$$\mu = \frac{1}{4} \left[\frac{Absolute\ rate}{M} + \frac{t}{T} + \left(\frac{\frac{Number\ of\ index\ changed}{in\ the\ count\ at\ t\text{-}th\ iteration}}{d} \right) z \right] , \quad (26)$$

where T indicates total time, M is constant, t is iteration index, d is a diameter. The solution update obtained in Eq. (26) is used for time-shifted optimal pilot scheduling.

Determination of best solution. The possible solutions are ranked based on the fitness function and the one that ranks the highest is the best solution.

Terminate. The best solutions are obtained iteratively until the maximum number of iterations are attained.

5. Results and Discussion

The proposed adaptive ESMO approach was analyzed using Matlab and was compared with existing methods based on achievable rate, SINR, and throughput by varying the number of users, the number of antennas and log-normal shadowing fading. The evaluated parameters include achievable rate, SINR, and throughput.

The achievable sum is used to optimize pilot information acquired from the channel dynamics and is:

$$A_r = B \times \log_2 \left(1 + \frac{P_s}{N + \sum_{i \in L} I^i} \right) , \quad (27)$$

where B indicates bandwidth, P_s refers to received signal power, N symbolizes background noise, and I^i indicates receiver interference.

SINR is the proportion of signal power and the sum of interference power from additional interfering signals with background noise:

$$SINR = \frac{\sigma}{\kappa + \chi} , \quad (28)$$

where σ indicate the incoming signal, κ represents interference power, and χ is a constant.

The throughput of the network is the rate of successful exchange of data through a communication channel within a specific period.

5.1. Experimental Results

Figure 6 shows the experimental results of the proposed adaptive ESMO with 10 and 15 users. The red triangle indicates BS, whereas the green circle represents mobile devices. Communication between users and BS involves the sending of pilots to evaluate channels. The user sends pilots at the same time, which results in pilot contamination. Thus, pilot contamination is managed by the adaptive ESMO model using time-shifted pilot based scheduling.
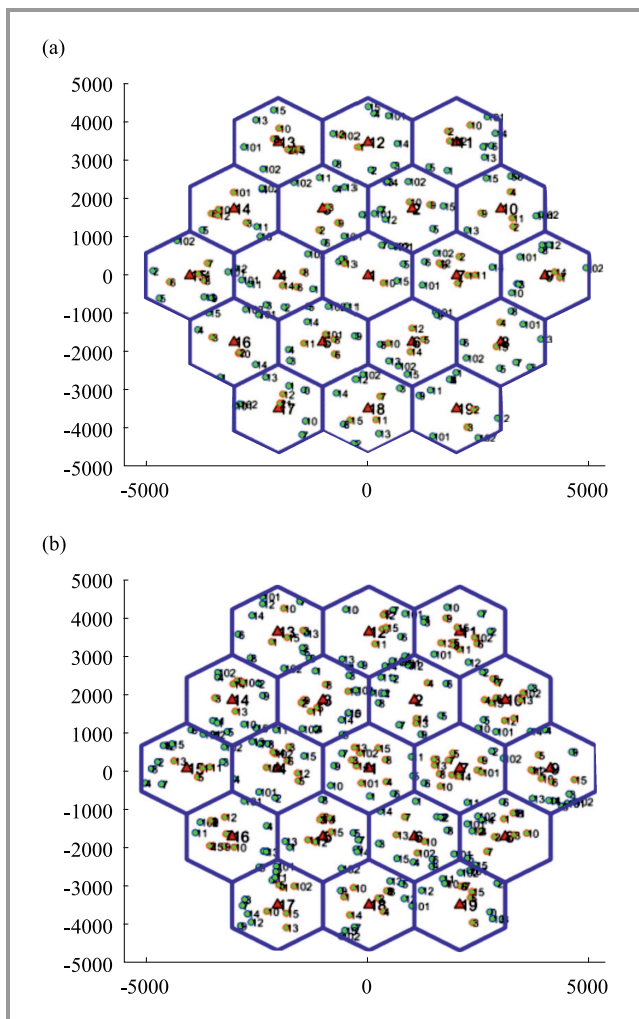
Fig. 6. Experimental results of the proposed adaptive ESMO using: (a) 10 users, (b) 15 users. (For color pictures see the digital version of the paper).

The remaining techniques used here for the purpose of the comparative analysis include: degradation-based scheduling from [26], MRT-ZF presented in [30], soft pilot reuse
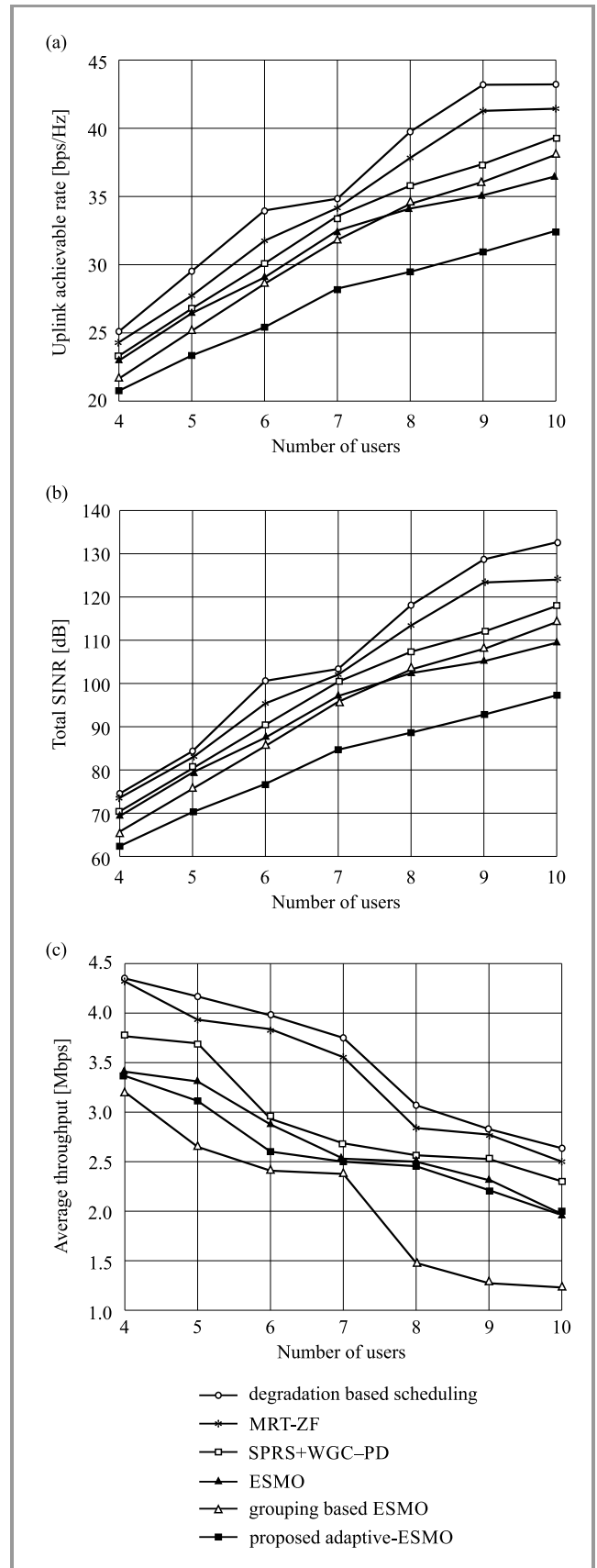
Fig. 7. Comparative analysis based on altering the number of users: (a) uplink achievable rate, (b) total SINR, and (c) average throughput.
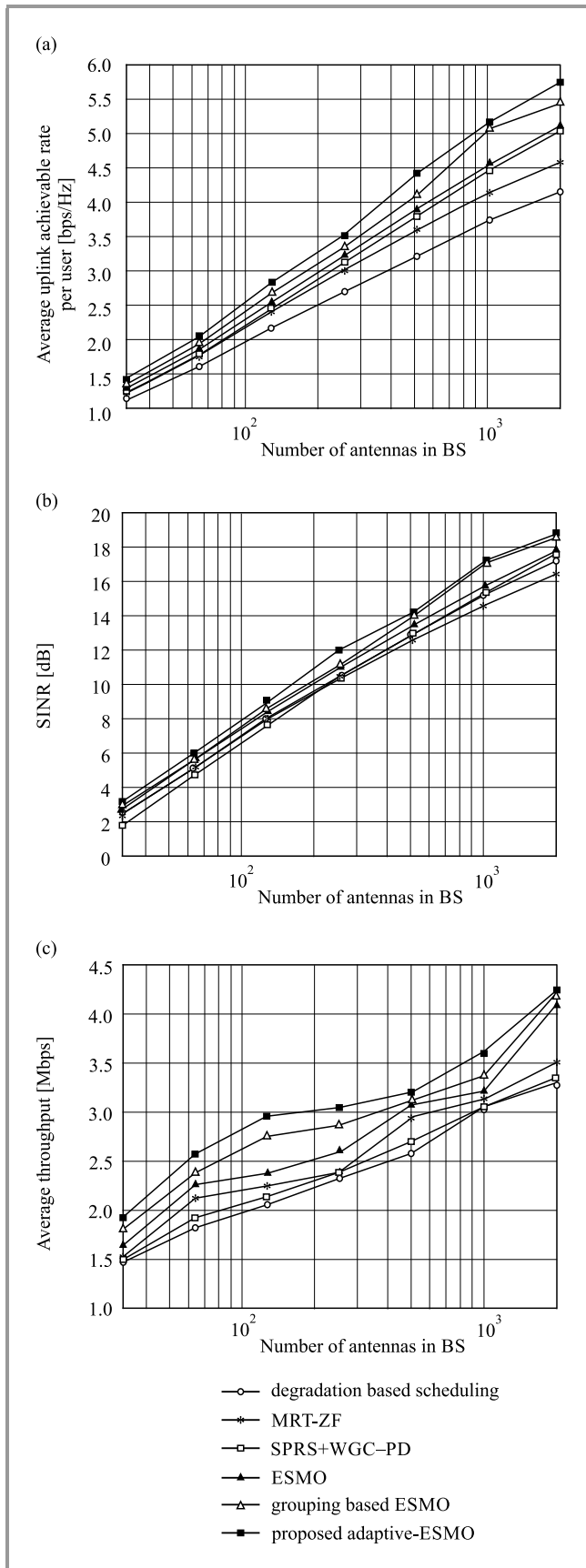
Fig. 8. Comparative analysis based on varying the number of the antennas in BS: (a) uplink achievable rate, (b) total SINR, and (c) average throughput.
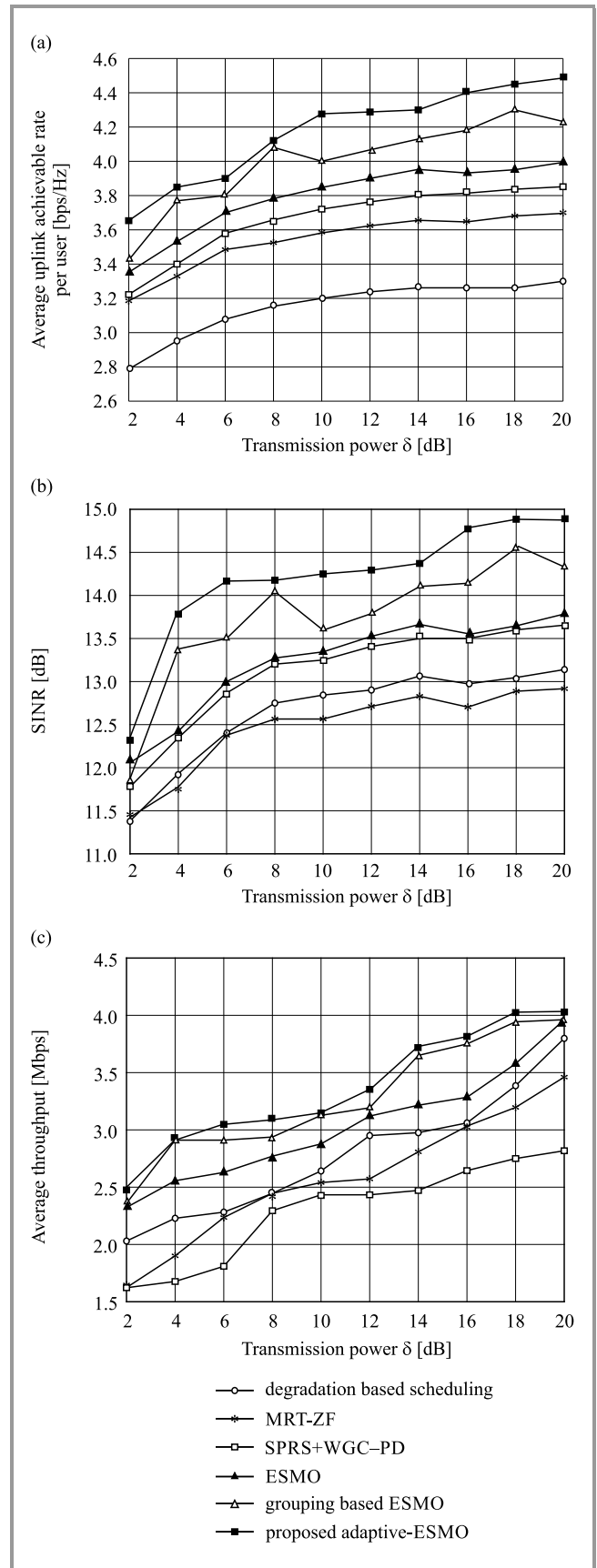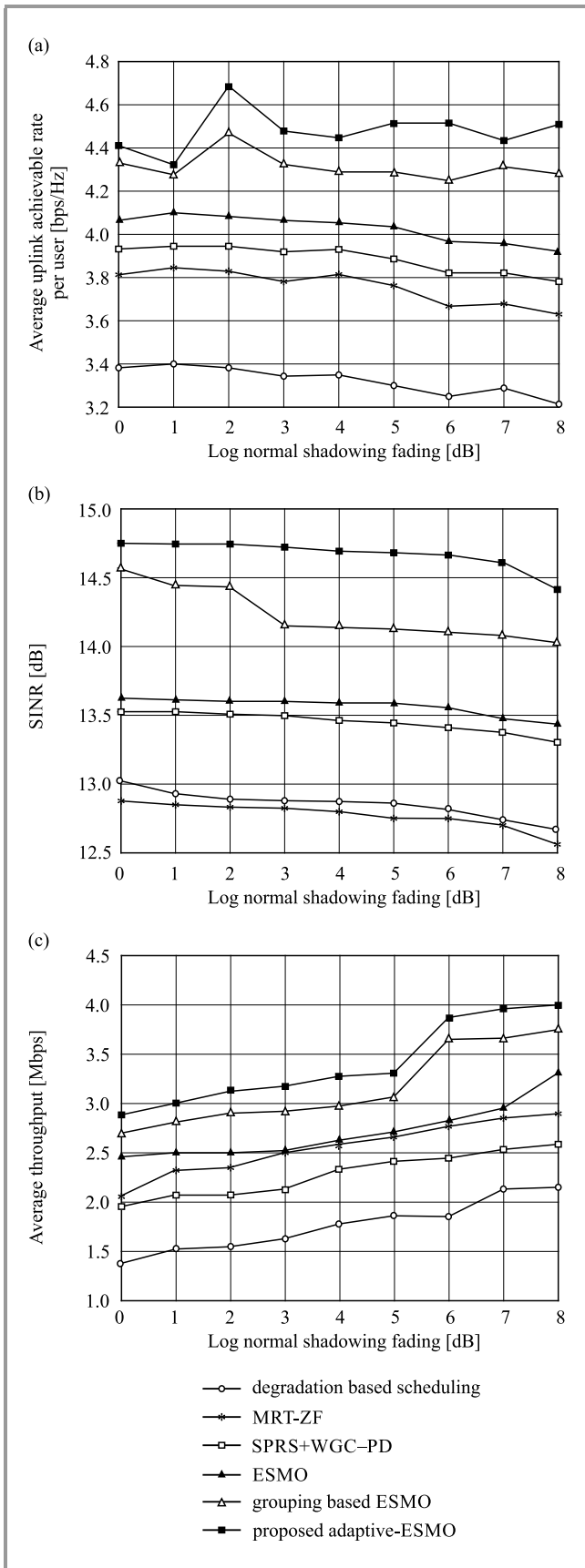
Fig. 9. Comparative analysis based on altering transmission power: (a) uplink achievable rate, (b) total SINR, and (c) average throughput.

Fig. 10. Comparative analysis based on altering log-normal shadowing fading: (a) uplink achievable rate, (b) total SINR, and (c) average throughput.

scheme + weighted coloring graph + pilot decontamination (SPRS+WGC-PD) from [31], ESMO, grouping-based ESMO and proposed adaptive ESMO.

Figure 7 illustrates the analysis of methods by altering the count of users considering the uplink achievable rate, total SINR, and average throughput.

Figure 8 shows an analysis of the different methods based on altering the number of antennas in BS, with the same criteria adopted.

Figure 9 presents an analysis of the methods based on altering the transmission power, while Fig. 10 shows alterations of log-normal shadowing fading, performed with the use of the same parameters as used in Figs. 7–8.

5.2. Discussion Concerning Achieved Results

Table 1 presents an analysis of the different methods considering the achievable uplink rate, total SINR, and average throughput. Considering the number of users, the maximum achievable rate of 43.084 bps/Hz is computed for adaptive ESMO. In contrast, the existing methods showed lower achievable rates. The maximum SINR of adaptive ESMO is 132.882 dB, whereas SINR of the other methods equals: degradation-based scheduling – 97.438 dB, MRT-ZF – 109.633 dB, SPRS+WGC-PD – 114.386 dB, ESMO – 118.176 dB, and grouping-based ESMO – 124.318 dB. The maximum average throughput computed for adaptive ESMO is 2.633 Mbps. Considering the number of antennas in BS, the proposed adaptive ESMO reached the maximum achievable rate of 5.758 bps/Hz, total SINR of 18.843 dB, and average throughput of 4.229 Mbps. For transmission power, adaptive ESMO reached the maximum achievable rate of 4.490 bps/Hz, total SINR of 14.874 dB, and average throughput of 4.022 Mbps. In the case of log-normal shadowing fading, adaptive ESMO reached the maximum achievable rate of 4.513 bps/Hz, total SINR of 14.409 dB, and average throughput of 4.017 Mbps.

6. Conclusion

In order to mitigate the adverse impact of pilot contamination, time-shifted pilot scheduling is performed using adaptive ESMO, a method incorporating adaptive tuning parameters into the ESMO algorithm. Here, the grouping of users is performed based on attributes including large-scale fading factor, SINR, and user distance. The sparse-FCM algorithm is used as well, helping categorize users as center users or edge users. The grouping of users is performed in such a way that the method effectively alleviates inappropriate grouping of users, and facilitates effective grouping, even under the worst channel conditions. Finally, pilot sequences are subjected to time-shifted pilot scheduling using the proposed adaptive ESMO algorithm in order to eliminate pilot contamination. The effectiveness of the proposed method was evaluated using specific parameters and revealed superior performance with

Table 1
Comparative data retrieved by the simulations

Parameter	Metric	Degradation-based scheduling	MRT-ZF	SPRS+WGC-PD	ESMO	Grouping-based ESMO	Proposed adaptive ESMO
Number of users	Achievable rate [bps/Hz]	32.368	36.419	37.998	39.257	41.298	**43.084**
	Total SINR [dB]	97.438	109.633	114.386	118.176	124.318	**132.882**
	Average throughput [Mbps]	1.945	1.221	1.951	2.280	2.495	**2.633**
Number of the antennas in BS	Achievable rate [bps/Hz]	4.157	4.582	5.055	5.120	5.448	**5.758**
	Total SINR [dB]	17.353	16.552	17.730	17.877	18.679	**18.843**
	Average throughput [Mbps]	3.294	3.515	3.347	4.076	4.194	**4.229**
Transmission power	Achievable rate [bps/Hz]	3.301	3.689	3.850	3.988	4.227	**4.490**
	Total SINR [dB]	13.127	12.915	13.658	13.791	14.315	**14.874**
	Average throughput [Mbps]	3.804	3.463	2.820	3.949	3.962	**4.022**
Log-normal shadowing fading	Achievable rate [bps/Hz]	3.227	3.642	3.785	3.927	4.286	**4.513**
	Total SINR [dB]	12.676	12.560	13.311	13.437	14.035	**14.409**

the highest achievable uplink rate of 43.084 bps/Hz, the highest SINR of 132.882 dB, and maximum throughput of 2.633 Mbps, respectively.

References

[1] I. A. Khan, "Robust signal detection scheme for 5G massive multiuser MIMO systems", *IEEE Trans. Veh. on Technol.*, vol. 67, pp. 9597–9604, 2018 (DOI: 10.1109/TVT.2018.2858922).

[2] F. Rusek *et al.*, "Scaling up MIMO: Opportunities and challenges with very large arrays", *IEEE Sig. Process.*, vol. 30, pp. 40–60, 2013 (DOI: 10.1109/MSP.2011.2178495).

[3] S. Biswas, J. Xue, F. A. Khan, and T. Ratnarajah, "Performance analysis of correlated massive MIMO systems with spatially distributed users", *IEEE Syst. J.*, vol. 12, pp. 1850–1861, 2016 (DOI: 10.1109/JSYST.2016.2594155).

[4] T. Marzetta, "Noncooperative cellular wireless with unlimited numbers of base station antennas", *IEEE Trans. on Wirel. Commun.*, vol. 9, no. 11, pp. 3590–3600, 2010 (DOI: 10.1109/TWC.2010.092810.091092).

[5] X. Zhu, L. Dai, and Z. Wang, "Graph coloring based pilot allocation to mitigate pilot contamination for multi-cell massive MIMO systems", *IEEE Commun. Lett.*, vol. 19, no. 10, pp. 1842–1845, 2015 (DOI: 10.1109/LCOMM.2015.2471304).

[6] W. A. Mahyiddin, P. A. Martin, and P. J. Smith, "Pilot contamination reduction using time-shifted pilots in finite massive MIMO systems", in *Proc. 2014 IEEE 80th Vehicular Technol. Conf. VTC2014-Fall 2014*, Vancouver, BC, Canada, 2014 (DOI: 10.1109/VTCFall.2014.6966130).

[7] H. Yin, D. Gesbert, M. C. Filippou, and Y. Liu, "Decontaminating pilots in massive MIMO systems", in *Proc. of IEEE Int. Conf. on Commun. ICC 2013*, Budapest, Hungary, 2013, pp. 3170–3175 (DOI: 10.1109/ICC.2013.6655031).

[8] R. Muller, L. Cottatellucci, and M. Vehkapera, "Blind pilot decontamination", *IEEE J. of Selec. Topics in Sig. Process.*, vol. 8, no. 5, pp. 773–786, 2014 (DOI: 10.1109/JSTSP.2014.2310053).

[9] R. Mochaourab, E. Björnson, and M. Bengtsson, "Pilot clustering in asymmetric massive MIMO networks", in *Proc. of the IEEE 16th Int. Worksh. on Sig. Process. Adv. in Wirel. Commun. SPAWC 2015*, Stockholm, Sweden, 2015 (DOI: 10.1109/SPAWC.2015.7227034).

[10] A. Ashikhmin and T. L. Marzetta, "Pilot contamination precoding in multi-cell large-scale antenna systems", in *Proc. of the IEEE Int. Symp. on Inform. Theory Proceedings ISIT 2012*, Cambridge, MA, USA, 2012, vol. 1, pp. 1137–1141, 2012 (DOI: 10.1109/ISIT.2012.6283031).

[11] L. Liangbin, A. Ashikhmin, and T. L. Marzetta, "Pilot contamination precoding for interference reduction in large-scale antenna systems", in *Proc. of the 51th Ann. Allerton Conf. on Commun., Control, and Comput. Allerton CCC 2013*, Monticello, IL, USA, 2013, vol. 2, no. 2, pp. 226–232 (DOI: 10.1109/Allerton.2013.6736528).

[12] T. M. Nguyen and L. B. Le, "Joint pilot assignment and resource allocation in multicell massive MIMO network: Throughput and energy efficiency maximization", in *Proc. of the IEEE Wirel. Commun. and Network. Conf. WCNC 2015*, New Orleans, LA, USA, 2015, vol. 9, pp. 393–398 (DOI: 10.1109/WCNC.2015.7127502).

[13] H. V. Cheng, E. Björnson, and E. G. Larsson, "Optimal pilot and payload power control in single-cell massive MIMO systems", *IEEE Trans. on Sig. Process.*, vol. 65, no. 9, pp. 2363–2378, 2017 (DOI: 10.1109/TSP.2016.2641381).

[14] H. T. Dao and S. Kim, "Pilot power allocation for maximizing the sum rate in massive MIMO systems", *IET Commun.*, vol. 12, no. 11, pp. 1367–1372, 2018 (DOI: 10.1049/iet-com.2017.1407).

[15] S. Jin *et al.*, "On massive MIMO zero-forcing transceiver using time-shifted pilots", *IEEE Trans. on Veh. Technol.*, vol. 65, no. 1, pp. 59–74, 2016 (DOI: 10.1109/TVT.2015.2391192).

[16] X. Xiong, B. Jiang, X. Gao, and X. You, "QoS-guaranteed user scheduling and pilot assignment for large-scale MIMO-OFDM systems", *IEEE Trans. on Veh. Technol.*, vol. 65, no. 8, pp. 6275–6289, 2015 (DOI: 10.1109/TVT.2015.2477683).

[17] X. Dai, "Optimal training design for linearly time-varying MIMO/OFDM channels modeled by a complex exponential basis expansion", *IET Commun.*, vol. 1, no. 5, pp. 945–953, 2007 (DOI: 10.1049/iet-com:20045301).

[18] B. Akgun, M. Krunz, and O. O. Koyluoglu, "Vulnerabilities of massive MIMO systems to pilot contamination attacks", *IEEE Trans. on Inform. Foren. and Secur.*, vol. 14, no. 5, pp. 1251–1263, 2018 (DOI: 10.1109/TIFS.2018.2876750).

[19] Y. Wu, C.-K. Wen, W. Chen, S. Jin, R. Schober, and G. Caire, "Data-aided secure massive MIMO transmission under the pilot contamination attack", *IEEE Trans. on Commun.*, vol. 67, no. 7, pp. 4765–4781, 2019 (DOI: 10.1109/TCOMM.2019.2907943).

[20] J. Fan, W. Li, and Y. Zhang, "Pilot contamination mitigation by fractional pilot reuse with threshold optimization in massive MIMO systems", *Digit. Sig. Process.*, vol. 78, pp. 197–204, 2018 (DOI: 10.1016/j.dsp.2018.02.011).

[21] O. A. Saraereh, I. Khan, B. M. Lee, and A. Tahat, "Efficient pilot decontamination schemes in 5G massive MIMO systems", *Electronics*, vol. 8, no. 1, pp. 55, 2019 (DOI: 10.3390/electronics8010055).

[22] I. E. Shaalan, A. A. Khattaby, and A. S. Dessouki, "A new joint TSPA/WGC pilot contamination reduction strategy based on exact graph coloring grouping algorithm", *IEEE Access*, vol. 7, pp. 150552–150564, 2019 (DOI: 10.1109/ACCESS.2019.2947665).

[23] Y. K. Hua and W. Chang, "Time shifted pilots scheme for full-duplex massive MIMO systems", *IEEE Trans. on Veh. Technol.*, vol. 68, no. 3, pp. 3022–3026, 2019 (DOI: 10.1109/TVT.2019.2893547).

[24] A. Salh, L. Audah, N. S. M. Shah, and S. A. Hamzah, "Mitigating pilot contamination for channel estimation in multi-cell massive MIMO systems", *Wirel. Pers. Commun.*, vol. 112, pp. 1643–1658, 2020 (DOI: 10.1007/s11277-020-07120-9).

[25] T. Wei, W. Feng, N. Ge, and J. Lu, "Optimized time-shifted pilots for maritime massive MIMO communication systems", in *Proc. 26th Wirel. and Opt. Commun. Conf. WOCC 2017*, Newark, NJ, USA, 2017 (DOI: 10.1109/WOCC.2017.7929003).

[26] Y. Wu, T. Liu, M. Cao, L. Li, and W. Xu, "Pilot contamination reduction in massive MIMO systems based on pilot scheduling", *EURASIP J. on Wirel. Commun. and Network.*, 2018, article no. 21, 2018 (DOI: 10.1186/s13638-018-1029-1).

[27] X. Chang, Q. Wang, Y. Liu, and Y. Wang, "Sparse regularization in fuzzy c-means for high-dimensional data clustering", *IEEE Trans. on Cybernet.*, vol. 47, no. 9, pp. 2616–2627, 2017 (DOI: 10.1109/TCYB.2016.2627686).

[28] G. G. Wang, S. Deb, and L. D. S. Coelho, "Elephant herding optimization", in *Proc. of 3rd Int. Symp. on Comput. and Business Intell. ISCBI 2015*, Bali, Indonesia, 2015 (DOI: 10.1109/ISCBI.2015.8).

[29] J. C. Bansal, H. Sharma, S. S. Jadon, and M. Clerc, "Spider monkey optimization algorithm for numerical optimization", *Memetic Comput.*, vol. 6, no. 1, pp. 31–47, 2014 (DOI: 10.1007/s12293-013-0128-0).

[30] J. Li, D. Wang, P. Zhu, J. Wang, and X. You, "Downlink spectral efficiency of distributed massive MIMO systems with linear beamforming under pilot contamination", *IEEE Trans. on Veh. Technol.*, vol. 67, no. 2, pp. 1130–1145, 2018 (DOI: 10.1109/TVT.2017.2733532).

[31] W. Yuan, X. Yang, and R. Xu, "A novel pilot decontamination scheme for uplink massive MIMO systems", *Procedia Comp. Sci.*, vol. 131, pp. 72–79, 2018 (DOI: 10.1016/j.procs.2018.04.187).

Ambala Pradeep Kumar received his B.Tech. degree and M.Tech. from Jawaharlal Nehru Technological University, Hyderabad, India, in 2008 and 2012, respectively. Between 2008 and 2016 he worked as an Assistant Professor at SR Engineering College, Warangal, India. He is currently pursuing Ph.D. at the Department of ECE, KU College of Engineering and Technology, Kakatiya University, Warangal, India. He published 6 papers in international journals and attended numerous conferences. His research interests are in the field of digital signal processing and wireless communications.

E-mail: ambalapradeepk@gmail.com
Department of ECE
KU College of Engineering and Technology
Kakatiya University
Warangal, Telangana, India

Tadisetty Srinivasulu is working as Professor and Dean at the Faculty of Engineering and Technology, Kakatiya University. He obtained M.Tech. from IIT Dhanbad, and Ph.D. from Kyushu University, Japan. He completed Proficiency Courses and received diplomas from IISc Bangalore, IIT Kharagpur, CEDTI Gorakhpur, NPA and NRDC New Delhi. The major administrative positions he held include Principal, Director, General Manager, Coordinator and Head of the Department. He published over 157 research papers in international journals and conference papers.

E-mail: drstadisetty@gmail.com
Department of ECE
KU College of Engineering and Technology
Kakatiya University
Warangal, Telangana, India